Post-flight Analysis of Atmospheric Properties from Mars 2020 Entry, Descent, and Landing

Soumyo Dutta*
NASA Langley Research Center, Hampton, VA 23681, USA

Christopher D. Karlgaard†
Analytical Mechanics Associates, Inc., Hampton, VA 23666, USA

David Kass‡, Michael Mischna§, and Gregorio G. Villar III¶
Jet Propulsion Laboratory, California Institute of Technology, Pasadena, CA 91109, USA

The Mars 2020 spacecraft landed the Perseverance rover and Ingenuity helicopter successfully in Jezero crater on Feb. 18, 2021. The entry, descent, and landing (EDL) sequence of the spacecraft largely leveraged the previous 2012 Mars Science Laboratory (MSL) mission. The atmospheric modeling approach for Mars 2020 was also borrowed from MSL. It consisted of two mesoscale atmospheric models of the target site during the Martian season of landing, and a statistical model of the pressure, density, temperature, and winds based on the mesoscale model data. This paper briefly describes the pre-flight atmospheric models used for Mars 2020, but focuses on the post-flight assessment of these models and comparison to near-landing day orbiter sounder and other onboard atmospheric measurements. Observations from post-flight analysis showed that density was under-predicted in the upper atmosphere, but within the altitudes covered by the mesoscale models, the pre-flight modeling matched post-flight results, including for quantities like wind velocities. Potential improvements to address the upper atmosphere and other deficiencies of the Mars 2020 pre-flight model are also discussed.

I. Introduction

The Mars 2020 mission delivered the largest and the most sophisticated rover in the form of the 1026 kg Perseverance to Jezero crater on Feb. 18, 2021. The entry, descent, and landing (EDL) sequence was very similar to the previous Mars Science Laboratory (MSL) mission which landed in 2012. Figure 1 shows the Mars 2020 concept of operations, with atmospheric entry, which is the start of the sensed atmosphere in the flight simulations, occurring at 125 km altitude above the Mars Orbiter Laser Altimeter (MOLA) defined surface, and landing occurring at approximately -2.5 km altitude below the MOLA datum 7 minutes later. The as-flown values shown are based on post-flight reconstruction from Refs. [1, 2] and discussions regarding comparison of as-flown values with predictions are addressed in Ref. [3].

Even though the average Mars atmospheric pressure is less than 1% of Earth's surface pressure, within the 130 km vertical column and approximately 600 km of horizontal distance of the entry flight path, atmospheric and aerodynamic forces play an important part in slowing the Mars 2020 spacecraft from interplanetary speeds down to a safe landing velocity. A sophisticated understanding of the Mars atmosphere is required in designing key EDL sequences for peak heating and deceleration, guided entry, parachute deploy, and both heatshield and backshell separation. Pre-flight models provide estimates of the landing site pressure, density, temperature, and wind speeds.

This paper will briefly describe the pre-flight atmospheric modeling efforts and analyses used during EDL operations to confirm the relevance of the pre-flight model. The majority of the paper will describe the post-flight analysis to develop an as-flown atmospheric model and comparison of the model to the pre-flight data. Finally, recommendations for updates to the atmospheric model for a future mission, such as Mars Sample Retrieval Lander, will be considered.

*Aerospace Engineer, Atmospheric Flight and Entry Systems Branch, 1 N. Dryden St., M/S 489, and Senior AIAA Member.
†Aerospace Engineer, Atmospheric Flight and Entry Systems Branch, 1 N. Dryden St., M/S 489, and Associate AIAA Fellow.
‡Scientist, 4800 Oak Grove Dr.
§Scientist, 4800 Oak Grove Dr. and Senior AIAA Member.
¶Systems Engineer, 4800 Oak Grove Dr.

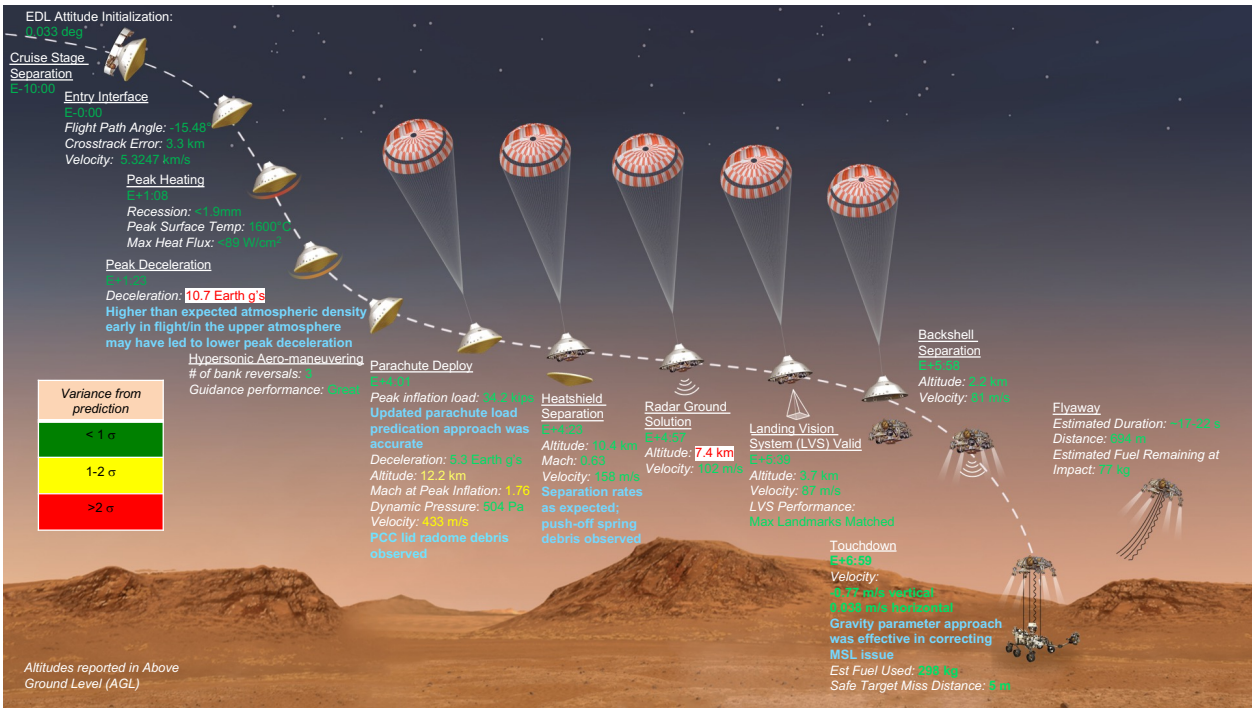

Fig. 1 Mars 2020 EDL concept of operations and as-flown conditions.

II. Pre-Flight Atmospheric Modeling

Mars 2020 borrowed MSL's plans for atmospheric modeling for pre-flight analysis. MSL identified that since the landing sites of interest were in locations with a large amount of terrain variation, vertical profiles of atmosphere simply over the landing site would not suffice. Profiles of atmospheric states varying in altitude and longitude would be required [4]. Additionally, the spacecraft was found to be sensitive to density variations below 30 km MOLA and to winds during the parachute phase of flight [5]. Above 30 km MOLA, density variations affected the closed-loop entry guidance performance, but had small effects on overall EDL metrics. Entry guidance was able to compensate for the different atmospheric properties and recover to nominal flight performance within 5-6 s of flight.

Due to the need for atmospheric models close to the surface, MSL had chosen to use two mesoscale models to provide pre-flight estimates of the atmosphere: Mars Mesoscale Model v5 (MMM5) [6] and Mars Regional Atmosphere Model System (MRAMS) [7]. The two model outputs were blended together to create one new model of the atmosphere, also known as a *Combo* profile [8].

The mesoscale and Combo modeling was already well-developed from MSL and thus this type of approach was used from the beginning of the Mars 2020 project. As seen in Figure 2, the Mars 2020 project ultimately analyzed twelve different sites with the mesoscale and Combo approach over the course of the project. Both mesoscale developers - MMM5 and MRAMS - were contracted to provide predictions of the landing site-specific Mars climate during the landing season.

The raw mesoscale data from the MMM5 and MRAMS models provide atmospheric properties and winds as three-dimensional tables that are functions of altitude, longitude, and latitude. Both models provide grids of different resolutions, spatial and temporal, and for a different number of Martian days or sols.

The three-dimensional spatial grid is reduced to two dimensions by querying the grid along the trajectory azimuth. This leads to a fixed latitude-to-longitude relationship and decreases one dimension of the data, which leads to a reduction in the size of the Combo tables used by the flight dynamics simulation. Pressure and temperature are interpolated in the altitude dimension with logarithmic interpolation, while linear interpolation is used for all other atmospheric properties in altitude and longitude dimensions.

For each mesoscale model, the mean and standard deviation of each atmospheric property are calculated from the interpolated data obtained from all simulated sols and within a 1.5 hour local mean solar time window around the target landing time. The mean and the standard deviation from each mesoscale model are then averaged to create final

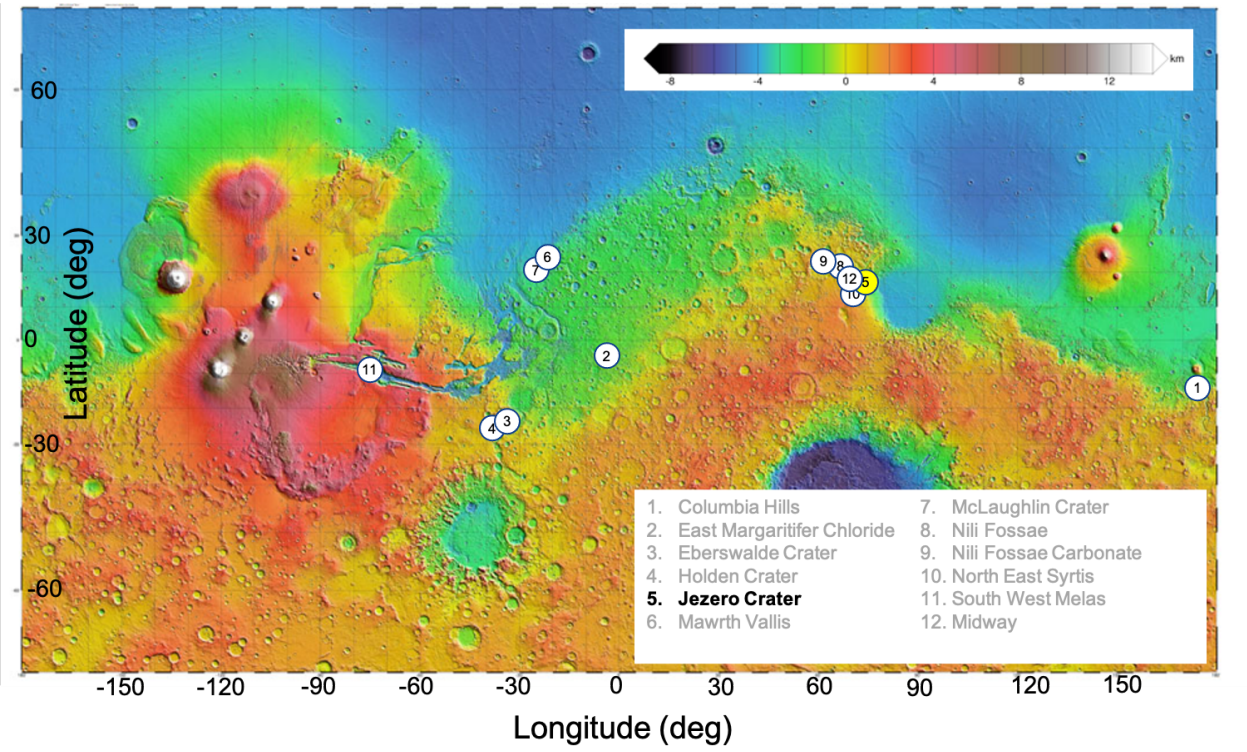

Fig. 2 Landing sites with mesoscale-based atmospheric models developed for Mars 2020.

values for the Combo profile, providing equal weight to each model. For the wind profiles, the standard deviations of the Combo model are defined to bound the worst-case scenario. Such a definition of wind variation stresses the EDL performance within the flight dynamics simulation. The mean Combo profile is still based on the average of the two mesoscale models, but the 3σ (or standard deviation) bounds of the Combo wind model at each vertical gridpoint are independently defined as the larger extreme of either model. Please see Ref. [9] for examples of how Combo wind models are created.

Unfortunately, the mesoscale models only provide a reliable atmospheric estimate up to 45-50 km MOLA altitude. EDL sensitivities to atmosphere are low above this region [5, 10, 11], but the pre-flight atmospheric model needs to define atmospheric properties up to the atmospheric interface at 125 km altitude MOLA. For both MSL and Mars 2020 pre-flight models, hydrostatic equilibrium, an isothermal assumption, and the ideal gas law are used to extend the atmospheric profile from the top of the mesoscale data set to the atmospheric interface. Winds are assumed to decrease linearly from their mesoscale value to 0 at 125 km MOLA altitude in the Mars 2020 model.

It is worth noting that the isothermal assumption used above 50 km MOLA altitude was known to be a poor assumption even before the flight. Temperature profiles in the mesosphere and thermosphere of Mars exhibit both positive and negative lapse rates and are seldom constant. However, due to lack of mesoscale model data in this region, the assumption was made to hold the temperature constant since it would be the mean effect between a positive and negative lapse rate. This assumption will be under more scrutiny in post-flight analysis.

Generally, the inputs and outputs of the Combo profile generation process from MSL were maintained for Mars 2020; however, based on lessons learned from MSL, three changes to the process itself were made.

First, the raw mesoscale data from each model were archived in a single place, rather than separately by the mesoscale modeling teams as done for MSL. Storing the raw data from all models in one place streamlined the process of performing reanalysis when procedural or other changes were implemented. Additionally, storing the data in one location maintained a chain of ownership.

Second, scripts used to process both mesoscale model outputs were standardized. For MSL, each model used independent processing scripts that often led to discrepancies between the outputs, requiring additional time to reconcile.

Finally and most significantly, adjustments were made to the Mars Global Reference Atmospheric Model (MarsGRAM

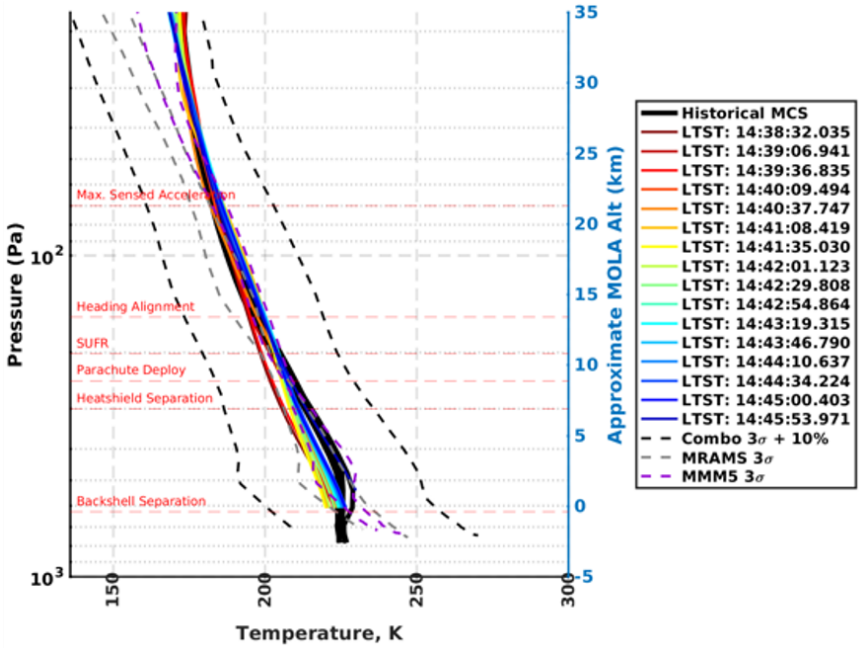

Fig. 3 Example of pressure and temperature profiles considered during EDL operations to understand the suitability of the pre-flight model in light of recent measurement data from Mars.

2005) code [12, 13] to accept the standard deviation values of density and horizontal winds from the mesoscale models. MarsGRAM is used to ingest the Combo profile into the EDL simulations and add high-frequency noise to the data. Previously, instead of the model-derived standard deviations, the ratio between the Combo profile standard deviation and the default MarsGRAM equivalent standard deviation was used at each level.

As this paper focuses on post-flight analysis, the readers can find further details of the pre-flight atmospheric modeling in Refs [9] and [14]. These references will describe how the atmospheric models are used by the flight mechanics simulations. Ref. [3] provides context of how the EDL predictions using the pre-flight model performed with respect to the flight data.

III. EDL Operations

During the weeks leading up to EDL operations, the pre-flight models were evaluated with Mars Climate Sounder (MCS) [15] data to understand if the current Mars conditions were similar to, or deviated from, the pre-flight Combo models. An example of a chart analyzed during operations is shown in Figure 3. The dashed lines represent the pre-flight MMM5, MRAMS, and Combo models, and the solid lines represent MCS data. The black solid lines are the mean historical MCS data from multiple Mars years and the colored lines are MCS profiles taken the previous day at different local true solar time (LTST). From these charts, the atmosphere team would determine if the pre-flight model was matching pre-landing expectations, especially in the region between 10 and 20 km where the system was most sensitive to density variations. There were no data about winds from MCS that allowed evaluation of the pre-flight wind models.

Figure 4 shows the evaluation used by the EDL team during operations.The EDL team compared the MCS retrievals with the pre-flight model in terms of atmospheric density, the atmospheric quantity to which EDL performance is most sensitive. The densities of all of the profiles and models were arbitrarily normalized to the MRAMS mean. The $\pm 3\sigma$ of the Combo profiles plus a 10% buffer, which is normally applied in flight dynamics simulations, served as the evaluation bounds. If the day-of-analysis MCS profiles were outside these bounds, the EDL team would decide if the pre-flight model needed to be adjusted. The criteria were narrowly tailored for a region between 10-20 km MOLA altitude, where EDL performance was most sensitive to density [5, 11].

Throughout EDL operations, the MCS profiles showed close agreement to the Combo profiles in the lower atmosphere where the EDL system was most sensitive. Due to the good agreement, the EDL team did not edit the pre-flight atmospheric model used for analysis. In pre-flight analysis, it was noted that at higher altitudes (40 km MOLA altitude)

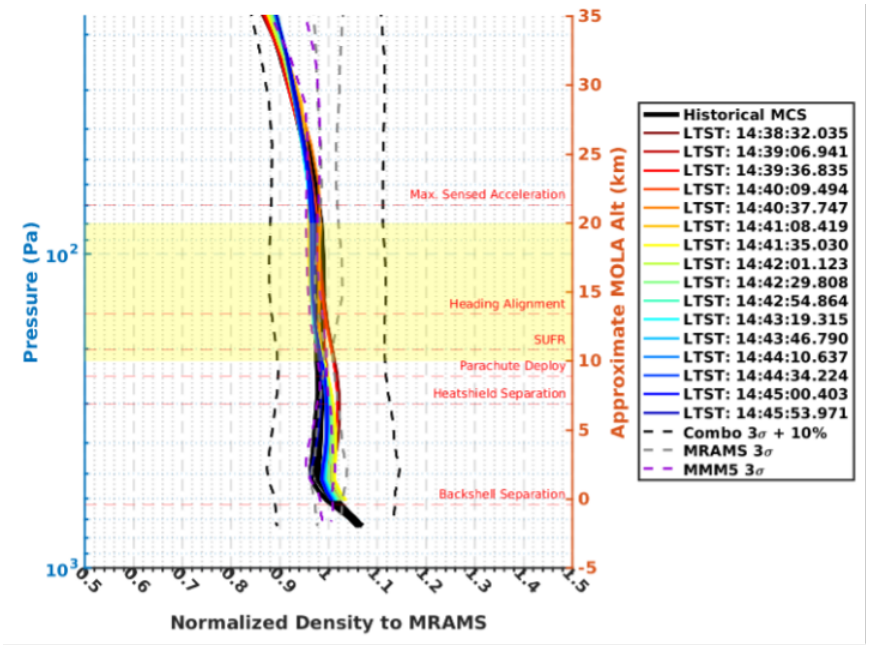

Fig. 4 Example of how the density criteria was analyzed during EDL operations to evaluate the suitability of the pre-flight model in light of recent measurement data from Mars.

the density profiles from the MCS instrument approached the bounds of the Combo model. However, due to less sensitivity to density at these higher altitudes, this observation was not seen as troubling.

During EDL operations, the team also monitored the dust opacity along a column via measurements from instruments on-board the Mars Reconnaissance Orbiter (MRO) and other orbital assets. Since Mars 2020's EDL utilized a landing vision system (LVS) camera to determine the vehicle's location, having an estimate of the dust opacity was crucial to predict the performance of the LVS. Discussion about the pre-flight modeling of dust opacity and monitoring of the data during EDL operations is covered in more detail in Refs. [9, 14].

IV. Post-Flight Analysis

After the Mars 2020 EDL was complete, there were four data sets available for the compilation of the as-flown EDL atmosphere.

The MCS profiles which were taken to support EDL operations were available as estimates of the upper atmosphere. The sounder profiles were taken near the EDL landing site, although due to the orbit of the MRO, which houses the MCS instrument, the tracks of the sounder profiles did not go directly over the landing site at every pass. Nevertheless, due to the adjacency of these profiles to the landing area of interest, these were a reasonable atmospheric estimate.

The capsule carried the Mars 2020 Entry Atmospheric Data System (MEADS) instrument as part of the Mars 2020 Entry, Descent, and Landing Instrumentation (MEDLI2) package [16]. The MEADS instrument took pressure measurements at several locations on the entry body, and these in-situ pressure measurements, along with pre-flight analysis of aerodynamic pressure distribution, were used to estimate freestream density, pressure, and temperature as well as uncertainties of these quantities. The instrument provided atmospheric estimates from approximately 70 km MOLA altitude to approximately the 10 km MOLA altitude where the parachute was deployed.

An additional on-board data source was the Mars Environmental Dynamics Analyzer (MEDA) instrument on the rover [17]. Although this instrument was not active during EDL, the sensor measurements of surface pressure at the local mean solar time of EDL from days following landing were used as estimates of the surface pressure.

Finally, profiles from the UK-based reanalysis tool, which incorporated observations from MCS and other on-orbit resources in a Global Circulation Model (GCM), were also available near the landing time and at the landing location. Using approximate 20 profiles from the this UKGCM tool [18–20], a mean temperature and pressure profile were created.

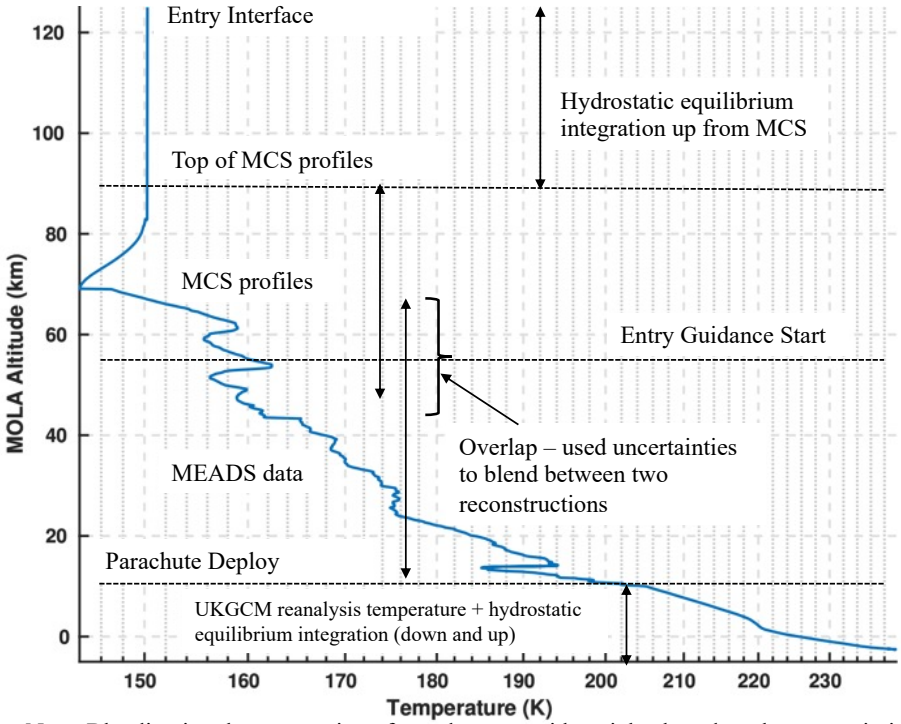

Note: Blending involves averaging of two data sets with weights based on the uncertainties

Fig. 5 Graphical representation of atmospheric data used for compilation of EDL atmosphere.

Figure 5 shows how the various data sets were used to compile a unified, as-flown estimate of the atmospheric profile for Mars 2020 EDL. The next sections describe the various segments of the post-flight atmospheric model.

For MSL's atmospheric reconstruction, the team also derived the atmospheric conditions from the inertial measurement unit (IMU) data while assuming nominal aerodynamic conditions. However, past experience has shown that such methods are typically less accurate since one is assuming perfect aerodynamic knowledge. The aerodatabase-based atmospheric reconstruction is not included in this paper, although Ref. [2] does include it and compares it to the atmospheric compilation method used in this paper.

A. Upper Atmosphere: MCS

There were no on-board measurements available above 70 km altitude MOLA. For this upper atmospheric region, the MCS profiles taken in days prior to EDL were used to estimate the as-flown atmosphere. The MCS data chosen were profiles taken around the latitude and longitude close to the entry interface and guidance start points, as seen in Figure 6, which were several hundred kilometers from the landing site. Only four series of profiles, named ATM009, ATM010, ATM014, and ATM018 in the convention used internally by the EDL team, were taken in the week of EDL and were geographically close to portions of the flight between entry interface and guidance start.

During EDL operations, MRO was oriented to have direct on-planet views for improved sounder profile quality. However, during actual EDL, MRO was re-oriented to support telemetry relay from the Mars 2020 spacecraft. Thus, the series of profiles taken shortly after landing, ATM018, did not have direct on-planet view that helps constrain the local surface needed for hydrostatic equilibrium. Due to the lack of alignment, these profiles were not recommended for post-flight analysis. The MCS profiles selected for post-flight analysis are shown in Figure 7. In total, there were 71 profiles, which were very consistent with each other and were averaged to generate the mean MCS profile used for the upper atmosphere post-flight estimate. The start of guidance is denoted in the figure as "range control start". This is the first location where atmosphere can sensibly affect the trajectory during EDL.

MCS profiles are not as accurate around 85 km MOLA and above. Thus, for the post-flight analysis, hydrostatic equilibrium, an isothermal assumption, and the ideal gas law were used to extend the atmospheric profile from the top of the reliable region of the MCS profiles to 125 km MOLA, which was the entry interface point.

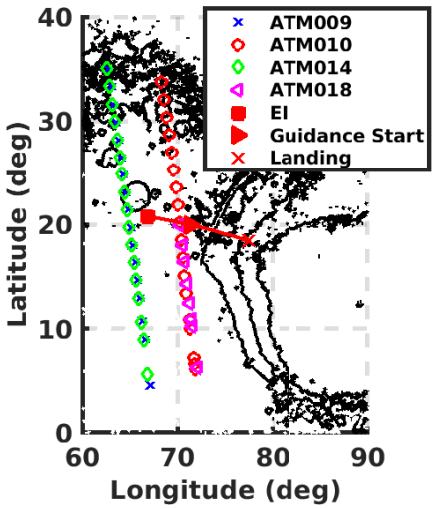

Fig. 6 Latitude and longitude of MCS profiles taken around the landing site near Feb. 18, 2021, with the red line representing the trajectory of Mars 2020.

B. Middle Atmosphere: MEADS

The MEADS data were available from approximately 70 km to 10 km MOLA, where the parachute was deployed. As described earlier, the pressure port data from the forebody of the vehicle allows one to estimate the freestream temperature, pressure, and density. Additionally, since the atmospheric relative velocity vector is known using the pressure port data, one can also estimate wind speeds if MEADS data are paired with the inertial velocity vector reconstructed using the on-board IMU.

The atmospheric estimation process using MEADS involves the use of an Extended Kalman Filter (EKF), which can combine various disparate on-board data, such as the IMU, MEADS, radar, LVS data, etc., to create a blended estimate of the vehicle trajectory and atmosphere. Since the EKF is a statistical filter, the reconstruction also produces an estimate

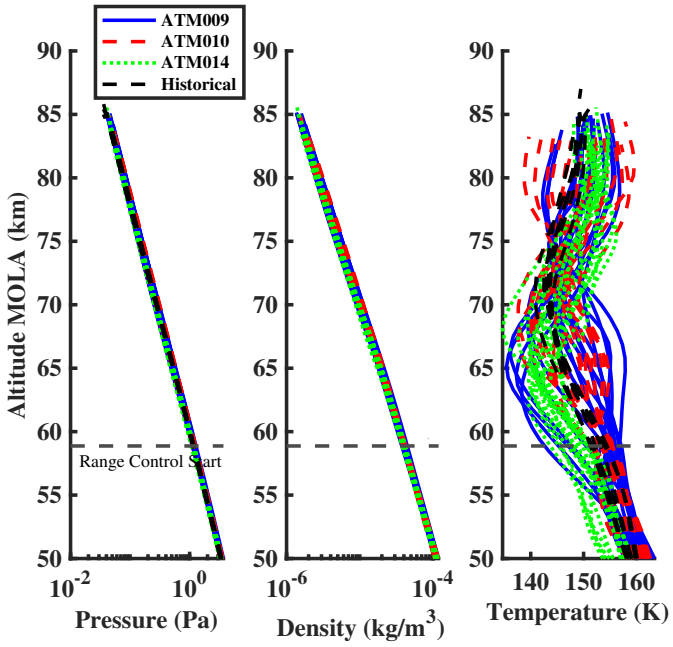

Fig. 7 MCS profiles taken around the landing site near Feb. 18, 2021.

of the uncertainty in the atmospheric quantities. The MEADS error model involves various components, such as errors in the calibration model used to convert voltage to engineering units, pneumatic lag in the transducers, and other sources of potential errors. References [2, 21] provide a more detailed description of the MEADS reconstruction process.

The middle atmospheric region had an overlapping region where both MCS profiles and MEADS data were available. Between 70 and 50 km MOLA altitude, the uncertainties of the MCS and MEADS atmospheric estimates were used to create a weighted average compiled estimate. The MCS uncertainties used for the post-flight analysis are derived from measurement data and variation of the many profiles averaged to create the upper atmosphere post-flight estimate. The MEADS uncertainties are also from the measurement data and are estimated during the EKF process.

C. Lower Atmosphere: UKGCM and MEDA Data

The MEADS instrumentation are calibrated to conditions that make the data less accurate after parachute deploy, which occurred around 10 km MOLA altitude. No other on-board measurements are available below this altitude and MCS profiles are not as accurate at altitudes so deep into the atmosphere. MEDA data are available at the surface for certain times within a few days of landing, but there is a gap in information between the last MEADS data and the surface-based MEDA data.

MSL had retuned one of its pre-flight profiles to provide atmospheric information between MEADS and the surface measurement [4]. However, for Mars 2020, UKGCM reanalysis data were available that were tuned to match day-of-flight conditions. The UKGCM provided a consistent model of the atmosphere rather than picking one pre-flight profile.

Thus, to bridge the gap between MEADS and MEDA data, UKGCM reanalysis data from around the landing site at 15:15:25 LTST were used. The temperature profile from the UKGCM tool was adjusted to match the last temperature data from MEADS, and hydrostatic equilibrium was used to integrate the MEDA surface pressure measurement to the middle atmosphere boundary at 10 km MOLA altitude.

D. Comparison of Post-Flight Analysis with Pre-Flight Model

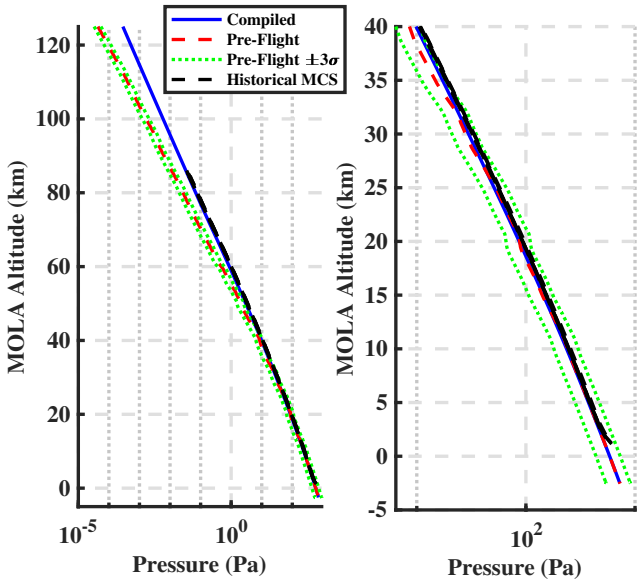

Fig. 8 Compiled pressure (blue) profile for Mars 2020 EDL along with pre-flight (red) and historical MCS (black) profiles.

The compiled Mars 2020 atmosphere is shown in Figures 8- 10 together with the pre-flight atmospheric estimate and the historical MCS profiles as a reference. The goal of the comparison is to see if the engineering models used pre-flight provided a good estimate of atmosphere experienced during EDL. The goal is not to see if the pre-flight models are good predictors of weather on Mars.

Pressure and density were underestimated by the pre-flight models above 40 km MOLA. This altitude range is outside the region of applicability of the mesoscale data (at around 45-50 km MOLA altitude) and is also where

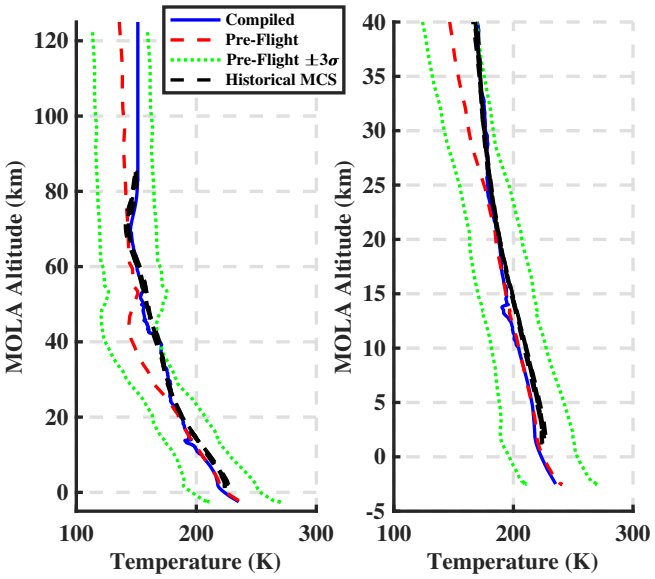

Fig. 9 Compiled (blue) temperature profile for Mars 2020 EDL along with pre-flight (red) and historical MCS (black) profiles.

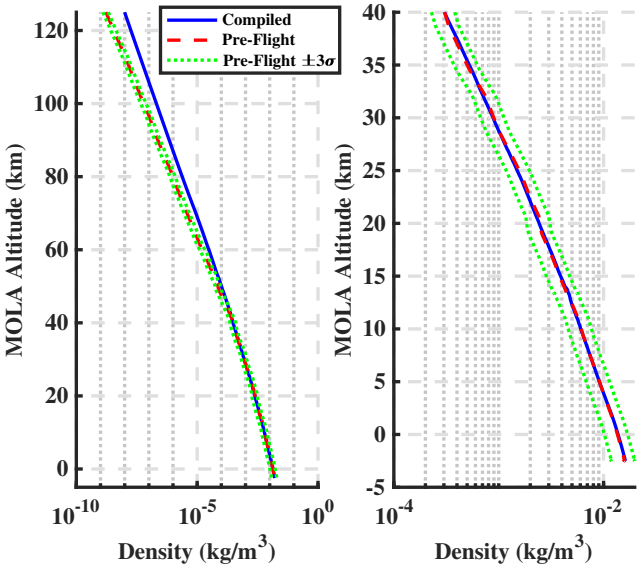

Fig. 10 Compiled (blue) density profile for Mars 2020 EDL along with pre-flight (red) profiles.

pre-flight models used hydrostatic equilibrium and an isothermal assumption to extrapolate the atmospheric data to the entry interface. During EDL operations, the team had observed that the historical MCS profiles and the MCS data from the day of analysis deviated from the mesoscale-based data around 30 km MOLA (see Figure 3). However, as EDL performance was not sensitive to the atmosphere at higher altitudes [5], no actions were taken. However, both the onboard measurement from MEADS and the MCS profiles chosen for the compiled atmosphere show a denser atmosphere than predicted.

Looking at the deviation of the density estimate in the post-flight analysis from the pre-flight model in Figure 11, one can see that the density was under-predicted by as much as 60% by the pre-flight model at the start of entry guidance. This discrepancy led to guidance starting 4 s (a 4σ+ event in Monte Carlo simulations) earlier than expected [3],

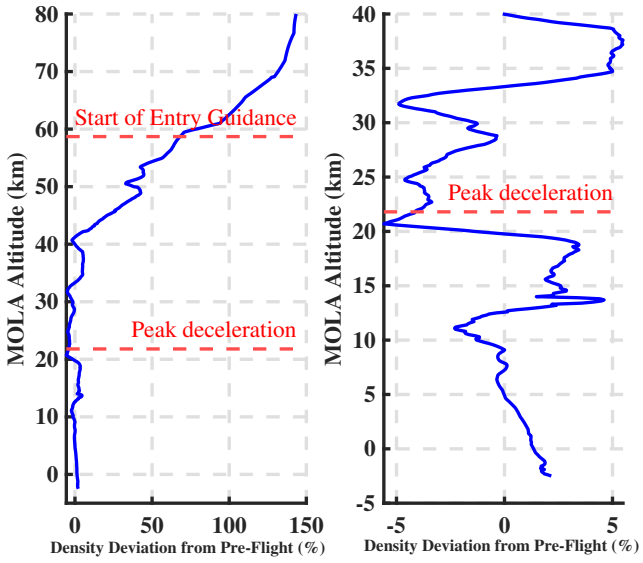

Fig. 11 Compiled atmosphere density deviation from pre-flight model.

although the overall effect of this start on the system performance was negligible and the vehicle corrected itself within 5-6 s [1–3]. However, the pre-flight model mis-predicting a key atmospheric parameter like density by such a large margin is concerning, especially in light of a density under-prediction of 20% by the pre-flight MSL model [4]. Systemic changes to the pre-flight modeling are needed in the upper atmospheric region, and this is discussed in Section V.

However, it should be noted that within the region of applicability of the mesoscale model (below 40 km MOLA altitude), the post-flight estimate and the pre-flight models are very consistent. Especially looking at pressure and density, the pre-flight model, the post-flight compiled atmosphere, and the historical MCS data are all are overlaid. The pre-flight model and its bounds encompass the flight estimate within the mesoscale model region. Looking at the density deviation chart (Figure 11), the difference in the pre-flight and post-flight models is well within the ±10% uncertainty applied in the flight dynamics simulations. Additionally, the difference between the pre-flight and post-flight models changes sign several times in the mesoscale region; it does not show a consistent bias, as was the case observed during MSL post-flight analysis [4].

The temperature profile from the post-flight analysis (Figure 9) correlates strongly with the historical MCS data. The divergence of the temperature profile between the pre-flight and post-flight model starts around 25 km MOLA altitude. This is the region where the two mesoscale models start to deviate from each other, as was seen in Figure 3. The MMM5 mesoscale model follows the historical MCS data and the compiled atmosphere more strongly than the other. However, in pre-flight models, both mesoscale models were given equal likelihood of predicting the conditions at the EDL landing site. Reliance on historical profiles, such as the MCS profiles, might alleviate such deviations in the future.

The pre-flight temperature profile does contain some structure that may be an artifact of the post-flight analysis. A temperature shear occurs near 14 km MOLA altitude in Figure 9 that appears to be non-physical. Improved calibration of the MEADS instrumentation reduced the magnitude of this shear, but did not completely remove the feature. Such features in as-flown temperature estimates have been observed in past Mars data [22, 23] and the causes have not been resolved. Regardless, the effect of this artifact is minor in the integrated pressure and density profiles (Figures 8 and 10).

The wind speed was estimated by the MEADS instrument between 10 and 50 km MOLA altitude. Figures 12 and 13 show the zonal (east/west) and meridional (north/south) wind estimates respectively overlaid on the pre-flight model. The wind estimates, which use the pre-flight model as an initial guess for the estimation algorithm, show remarkable similarity to the mean pre-flight profile. This is in contrast to MSL, where the same procedure was used but the estimated winds were very different from the pre-flight mean [4]. The estimated wind profiles for Mars 2020 show a small level of noise between 10-15 km MOLA altitude, but this is the region where the spacecraft is in horizontal flight and is going over a large swath of terrain; thus, it is expected that the wind speed estimates will vary within a small change in altitude during horizontal flight. Nevertheless, even in this region, the wind estimates are within the bounds of the pre-flight model. Improvements in mesoscale modeling and tuning of the models since MSL contributed to their

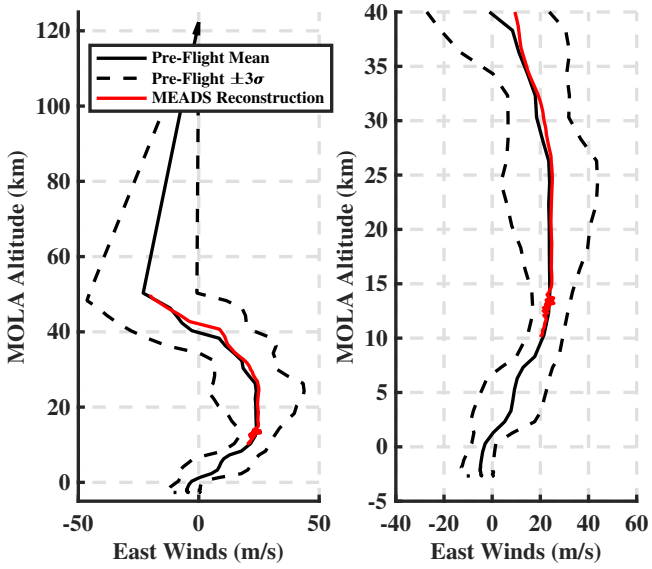

Fig. 12 Compiled east/west (zonal) wind profile for Mars 2020 EDL.

good performance in the region of their applicability.

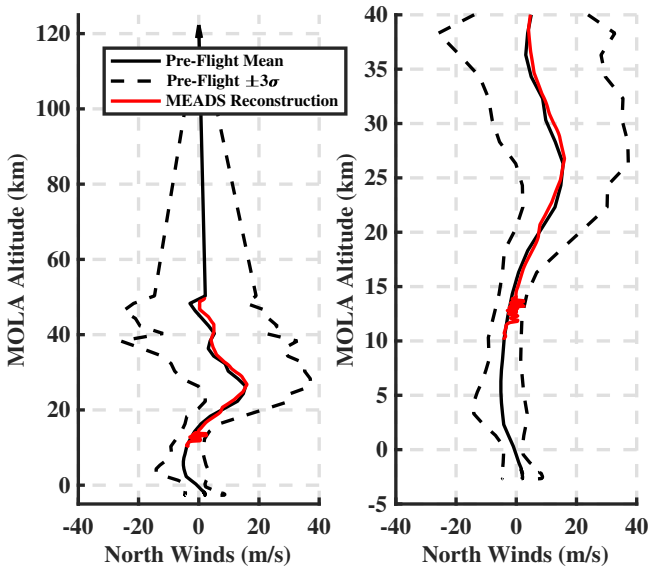

Fig. 13 Compiled north/south (meridional) wind profile for Mars 2020 EDL.

V. Recommendations for Future Atmospheric Models

In the past, Mars EDL missions have landed in unique landing sites. Thus, post-flight analysis of atmospheric models for Mars is usually not applicable to other missions. However, Mars 2020's model may be used for future missions, in particular the upcoming Mars Sample Retrieval Lander, which is designed to land in the same season and location as Mars 2020. Hence, lessons learned from Mars 2020, and improvements to its pre-flight atmospheric model, are relevant for future flight opportunities.

The pre-flight Mars 2020 atmospheric profile did not predict higher density at guidance start close to 60 km MOLA altitude [3]. Recall that the mesoscale data were only available up to a region of 45-50 km altitude MOLA, above which the atmospheric profiles were extrapolated using an isothermal assumption and hydrostatic equilibrium. However, for a future mission, one could use MCS historical averages to bridge between the top of the mesoscale region (45-50 km) to the top of the trusted MCS area (90 km). Historical averages are available now from many different Mars years, and have shown great agreement with post-flight data for Mars 2020, as seen in Figures 8-9. Instead of an isothermal assumption from 50 km up to 125 km MOLA altitude, the MCS historical temperature profiles can be used to extend the atmospheric model up to at least 90 km MOLA altitude, after which an isothermal assumption can once again be used to 125 km MOLA altitude. Such a procedure could prevent an under-prediction of density similar to the one recorded in Mars 2020 and MSL [4].

Post-flight analysis also showed that the peak sensed deceleration was overestimated by the pre-flight models. Ref. [3] describes how small changes in the lapse rate and scale height of the atmospheric model used in flight mechanics simulations can recreate the as-flown value of the sensed deceleration. Peak sensed acceleration occurs around 20 km MOLA altitude, which is where pre-flight predictions from the two mesoscale models began to diverge (see Figure 3). Since the Combo model averages both of the mesoscale models equally, the averaging adds new structure and inflection points to the derivative of the temperature (lapse rate) and pressure (scale height) profiles not present in either original mesoscale data. The specifics of how to address this issue is still under analysis, but may involve leveraging the independent historical MCS data that are available in this region of the atmosphere.

VI. Summary

The Mars 2020 spacecraft successfully landed at Jezero crater on Feb. 18, 2021. The Entry, Descent, and Landing trajectory was designed using pre-flight estimates of the seasonal weather at Jezero crater. These estimates were based on mesoscale models that were combined to create a Combo profile. After EDL, onboard data and Mars Climate Sounder retrievals were used to construct a compiled atmospheric profile for Mars 2020. Upon comparison with the pre-flight estimate, the upper atmospheric density was underestimated, which manifested in the flight when entry guidance started 4 seconds early. However, for much of the region where EDL is sensitive to the atmosphere, 40 km altitude and lower, the compiled atmosphere closely matched the pre-flight estimate. Updates to the pre-flight model to support follow-on missions could involve incorporating historical data to address zones where extrapolation of the mesoscale data took place.

Acknowledgments

A portion of this work was carried out at the Jet Propulsion Laboratory, California Institute of Technology, under a contract with the National Aeronautics and Space Administration (80NM0018D0004). The authors would like to acknowledge the help of the many members of the Mars 2020 Council of Atmospheres, the peer reviewers for the multiple Council of Atmosphere reviews, and the members of the Mars 2020 EDL team that shared their insight during the design and reconstruction efforts. The authors want to specifically thank Dr. Stephen Lewis of the Open University who provided the mean UKGCM profiles near the landing site from his reanalysis results.

References

[1] Serrichio, F., San Martin, A., Brugarolas, P., and Casoliva, J., "The Mars 2020 Perseverance Navigation Filter," AAS 21-539*, AAS/AIAA Astrodynamics Specialist Conference,* Big Sky, MT, 2021.

[2] Karlgaard, C., Schoenenberger, M., Dutta, S., and Way, D., "Mars Entry, Descent, and Landing Instrumentation 2 Trajectory and Atmosphere Reconstruction," *AIAA SciTech 2022, AIAA Atmospheric Flight Mechanics Conference,* San Diego, CA, 2022.

[3] Way, D., Dutta, S., Zumwalt, C., and Blette, D., "Assessment of the Mars 2020 Entry, Descent, and Landing Simulation," *AIAA SciTech 2022, AIAA Atmospheric Flight Mechanics Conference,* San Diego, CA, 2022.

[4] Chen, A., Cianciolo, A., Vasavada, A., Karlgaard, C., Barnes, J., Cantor, B., Kass, D., Rafkin, S., and Tyler, D., "Reconstruction of Atmospheric Properties from Mars Science Laboratory Entry, Descent, and Landing," *Journal of Spacecraft and Rockets*, Vol. 41, No. 4, 2014, pp. 1062–1075. doi:10.2514/1.A32708.

[5] Chen, A., Vasavada, A., Cianciolo, A., Barnes, J., Tyler, D., Rafkin, S., Hinson, D., and Lewis, S., "Atmospheric Risk

Assessment for the Mars Science Laboratory Entry, Descent, and Landing System," IEEEAC 1153, *IEEE Aerospace Conference,* Big Sky, MT, 2010.

[6] Tyler Jr., D., Barnes, J., and Skyllingstad, E., "Mesoscale and large-eddy simulation model studies of the Martian atmosphere in support of Phoenix," *Journal of Geophysical Research*, Vol. 113, No. E00A12, 2008, pp. 1–27. doi:10.1029/2007JE003012.

[7] Rafkin, S., Haberle, R., and Michaels, T., "The Mars Regional Atmospheric Modeling System: Model Description and Selected Simulations," *Icarus*, Vol. 151, 2001, pp. 228–256. doi:10.1006/icar.2001.6605.

[8] Cianciolo, A., Way, D., Powell, R., and Chen, A., "Mesoscale Atmosphere Model Implementation into Mars Science Laboratory Performance Simulations," *Lunar and Planetary Institute Third International Workshop on the Mars Atmosphere: Modeling and Observations*, 2008.

[9] Mischna, M., Villar, G., Kass, D., Dutta, S., Rafkin, S., Tyler, D., Barnes, J., Cantor, B., Lewis, S., Hinson, D., Pla-Garcia, J., Kleinbohl, A., and Karlgaard, C., "Pre- and Post-Entry, Descent and Landing Assessment of the Martian Atmosphere for the Mars 2020 Rover," *The Planetary Science Journal*, submitted.

[10] Mendeck, G., and McGrew, L., "Entry Guidance Design and Postflight Performance for 2011 Mars Science Laboratory Mission," *Journal of Spacecraft and Rockets*, Vol. 51, No. 4, 2014, pp. 1094–1105. doi:10.2514/1.A32737.

[11] Dutta, S., and Way, D., "Comparison of the Effects of Velocity and Range Triggers on Trajectory Dispersions for the Mars 2020 Mission," AIAA 2017-0245, *AIAA Atmospheric Flight Mechanics Conference,* Grapevine, TX, 2017.

[12] Justh, H., and Justus, C., "Mars Global Reference Atmospheric Model (Mars-GRAM 2005) applications for Mars Science Laboratory mission site selection process," *7th International Conference on Mars,* No. 3291, 2007.

[13] Justh, H., Justus, C., and Ramey, H., "The Next Generation of Mars-GRAM and its Role in the Autonomous Aerobraking Development Plan," AAS 11-478*, AAS/AIAA Astrodynamics Specialists Conference,* Girdwood, AK, 2011.

[14] Chen, A., et al., "Mars 2020 Entry, Descent, and Landing As-Flown Report," Tech. rep., Jet Propulsion Laboratory, Pasadena, CA, 2021, in work.

[15] Kleinböhl, A., Schofield, J. T., Kass, D. M., Abdou, W. A., Backus, C., Sen, B., Shirley, J. H., Gregory Lawson, W., Richardson, M. I., Taylor, F. W., Teanby, N. A., , and McCleese, D. J., "Mars Climate Sounder Limb Profile Retrieval of Atmospheric Temperature, Pressure, Pressure, and Dust and Water Ice Opacity," *Journal of Geophysical Research*, Vol. E10, 2009, pp. 1–30. doi:10.1029/2009JE003358.

[16] Hwang, H., Bose, D., White, T., Wright, H., , Schoenenberger, M., Kuhl, C., Trombetta, D., Santos, J., Oishi, T., Karlgaard, C., Mahzari, M., and Pennigton, S., "Mars 2020 Entry, Descent, and Landing Instrumentation (MEDLI2)," AIAA 2016-3536, *46th AIAA Thermophysics Conference,* Washington DC, 2016.

[17] Rodriguez-Manfredi, J. A., de la Torre Juarez, M., and et al, "The Mars Environmental Dynamics Analyzer, MEDA. A Suite of Environmental Sensors for the Mars 2020 Mission," *Space Science Reviews*, Vol. 217, No. 48, 2021, pp. 1–86. doi:10.1007/s11214-021-00816-9.

[18] Lewis, S., and Barker, P., "Atmospheric tides in a Mars general circulation model with data assimilation," *Advances in Space Research*, Vol. 36, 2005, pp. 2162–2168. doi:10.1016/j.asr.2005.05.122.

[19] Lewis, S., Read, P., Conrath, B., Pearl, J., and Smith, M., "Assimilation of Thermal Emission Spectrometer atmospheric data during the Mars Global Surveyor aerobraking period." *Icarus*, Vol. 192, 2007, pp. 327–347. doi:10.1016/j.icarus.2007.08.009.

[20] Holmes, J., Lewis, S., and Patel, M., "OpenMARS: A global record of martian weather from 1999 to 2015," *Planetary and Space Science*, Vol. 188, 2020. doi:10.1016/j.pss.2020.104962.

[21] Karlgaard, C., Kutty, P., Schoenenberger, M., Munk, M., Little, A., Kuhl, C., and Shidner, J., "Mars Science Laboratory Entry Atmospheric Data System Trajectory and Atmosphere Reconstruction," *Journal of Spacecraft and Rockets*, Vol. 51, No. 4, 2014, pp. 1029–1047. doi:10.2514/1.A32770.

[22] Karlgaard, C., and Tynis, J., "Mars Phoenix EDL Trajectory and Atmosphere Reconstruction Using NewSTEP," Tech. rep., NASA Technical Memorandum, *NASA/TM–2019–220282*, 2019.

[23] Karlgaard, C., Korzun, A., Schoenenberger, M., Bonfiglio, E., Kass, D., and Grover, M., "Mars InSight Entry, Descent, and Landing Trajectory and Atmosphere Reconstruction," *Journal of Spacecraft and Rockets*, Vol. 58, No. 3, 2021, pp. 865–878. doi:10.2514/1.A34913.

Appendix: Post-flight Estimate of the As-Flown Mars 2020 Atmosphere.

MOLA Altitude (m)	Temperature (K)	Pressure (Pa)	Density (kg/m^3)	East Wind (m/s)	North Wind (m/s)
-2500	235.298	7.247e+02	1.614e-02	-5.942	1.979
-2000	232.693	6.951e+02	1.566e-02	-6.005	1.850
-1500	230.089	6.664e+02	1.518e-02	-5.942	1.449
-1000	227.611	6.385e+02	1.470e-02	-5.646	1.020
-500	225.431	6.116e+02	1.422e-02	-4.989	0.542
0	223.357	5.856e+02	1.374e-02	-4.161	0.043
500	221.424	5.605e+02	1.327e-02	-2.861	-0.532
1000	219.739	5.362e+02	1.279e-02	-0.663	-1.255
1500	218.521	5.129e+02	1.230e-02	1.755	-2.040
2000	217.884	4.905e+02	1.180e-02	4.247	-2.952
2500	217.642	4.690e+02	1.129e-02	6.527	-3.860
3000	217.372	4.484e+02	1.081e-02	7.845	-4.402
3500	216.964	4.287e+02	1.036e-02	8.744	-4.799
4000	216.553	4.099e+02	9.922e-03	9.176	-5.023
4500	216.141	3.919e+02	9.503e-03	9.485	-5.158
5000	215.383	3.746e+02	9.116e-03	9.759	-5.192
5500	214.443	3.580e+02	8.751e-03	10.056	-5.170
6000	213.469	3.421e+02	8.400e-03	10.555	-5.072
6500	212.491	3.268e+02	8.062e-03	11.281	-4.929
7000	211.469	3.122e+02	7.738e-03	12.488	-4.727
7500	210.278	2.981e+02	7.431e-03	13.957	-4.513
8000	209.057	2.846e+02	7.136e-03	15.608	-4.352
8500	207.828	2.717e+02	6.851e-03	17.303	-4.216
9000	206.593	2.592e+02	6.577e-03	18.597	-4.044
9500	205.374	2.473e+02	6.311e-03	19.484	-3.937
10000	204.360	2.358e+02	6.049e-03	19.952	-4.022
10500	202.162	2.248e+02	5.830e-03	20.960	-3.587
11000	200.637	2.143e+02	5.597e-03	21.605	-3.703
11500	199.637	2.041e+02	5.360e-03	22.069	-3.171
12000	198.995	1.944e+02	5.122e-03	21.819	-0.950
12500	197.321	1.852e+02	4.919e-03	21.189	-2.533
13000	193.530	1.762e+02	4.773e-03	23.887	0.455
13500	191.823	1.676e+02	4.579e-03	22.386	-1.877
14000	195.754	1.593e+02	4.265e-03	22.765	-0.026
14500	193.639	1.515e+02	4.102e-03	24.079	-0.023
15000	193.957	1.442e+02	3.896e-03	24.718	0.537
15500	193.967	1.371e+02	3.706e-03	24.758	1.090
16000	192.025	1.304e+02	3.561e-03	24.675	1.629
16500	191.256	1.240e+02	3.399e-03	24.539	2.184
17000	190.404	1.179e+02	3.246e-03	24.585	2.899
17500	190.078	1.121e+02	3.090e-03	24.616	3.783
18000	189.430	1.065e+02	2.947e-03	24.655	4.719
18500	189.215	1.012e+02	2.803e-03	24.702	5.654
19000	188.848	9.615e+01	2.669e-03	24.657	6.550
19500	188.308	9.135e+01	2.543e-03	24.565	7.240

MOLA Altitude (m)	Temperature (K)	Pressure (Pa)	Density (kg/m^3)	East Wind (m/s)	North Wind (m/s)
20000	187.220	8.677e+01	2.429e-03	24.487	7.500
20500	186.312	8.240e+01	2.318e-03	24.425	7.762
21000	185.475	7.823e+01	2.211e-03	24.417	8.468
21500	184.718	7.426e+01	2.107e-03	24.464	9.471
22000	183.454	7.047e+01	2.013e-03	24.525	10.394
22500	182.320	6.685e+01	1.922e-03	24.595	11.316
23000	181.305	6.340e+01	1.833e-03	24.670	12.122
23500	180.152	6.010e+01	1.749e-03	24.752	12.792
24000	178.883	5.697e+01	1.669e-03	24.857	13.491
24500	178.584	5.397e+01	1.584e-03	24.948	14.230
25000	178.520	5.114e+01	1.502e-03	24.925	14.803
25500	177.970	4.845e+01	1.427e-03	24.806	15.155
26000	178.263	4.590e+01	1.350e-03	24.605	15.463
26500	178.037	4.349e+01	1.280e-03	24.457	15.825
27000	178.427	4.120e+01	1.210e-03	24.152	15.842
27500	178.655	3.904e+01	1.145e-03	23.624	15.418
28000	177.923	3.699e+01	1.090e-03	23.144	15.001
28500	178.204	3.505e+01	1.031e-03	22.716	14.610
29000	178.248	3.321e+01	9.766e-04	22.398	14.159
29500	178.156	3.147e+01	9.258e-04	22.065	13.404
30000	176.427	2.981e+01	8.857e-04	21.535	12.464
30500	176.480	2.823e+01	8.385e-04	21.213	11.633
31000	176.298	2.674e+01	7.949e-04	20.852	10.883
31500	176.102	2.532e+01	7.536e-04	20.303	10.373
32000	175.618	2.398e+01	7.156e-04	19.636	9.757
32500	175.263	2.270e+01	6.789e-04	18.811	8.948
33000	174.900	2.149e+01	6.441e-04	17.851	8.163
33500	173.556	2.034e+01	6.144e-04	16.855	7.495
34000	172.548	1.925e+01	5.847e-04	15.881	6.812
34500	172.232	1.821e+01	5.541e-04	14.979	6.134
35000	172.166	1.722e+01	5.243e-04	14.275	5.725
35500	172.070	1.629e+01	4.962e-04	13.599	5.443
36000	171.746	1.541e+01	4.703e-04	12.911	5.148
36500	171.475	1.457e+01	4.455e-04	12.222	4.842
37000	170.661	1.378e+01	4.233e-04	11.773	4.622
37500	170.506	1.303e+01	4.005e-04	11.465	4.438
38000	170.579	1.232e+01	3.786e-04	11.187	4.266
38500	170.833	1.165e+01	3.574e-04	10.923	4.109
39000	170.866	1.101e+01	3.379e-04	10.515	4.216
39500	170.561	1.042e+01	3.201e-04	9.994	4.446
40000	169.671	9.848e+00	3.042e-04	9.437	4.681
40500	168.353	9.308e+00	2.898e-04	8.862	4.920
41000	167.559	8.793e+00	2.751e-04	6.863	5.027
41500	167.051	8.306e+00	2.606e-04	3.798	5.029
42000	165.530	7.843e+00	2.484e-04	0.736	5.018
42500	160.938	7.399e+00	2.410e-04	-2.349	5.008
43000	160.428	6.972e+00	2.278e-04	-4.401	4.747
43500	160.061	6.569e+00	2.151e-04	-5.561	4.259

MOLA Altitude (m)	Temperature (K)	Pressure (Pa)	Density (kg/m^3)	East Wind (m/s)	North Wind (m/s)
44000	159.981	6.189e+00	2.028e-04	-6.726	3.834
44500	158.994	5.830e+00	1.922e-04	-7.939	3.411
45000	158.858	5.491e+00	1.812e-04	-9.251	2.832
45500	157.095	5.170e+00	1.725e-04	-10.639	2.092
46000	157.325	4.866e+00	1.621e-04	-12.018	1.358
46500	156.768	4.580e+00	1.531e-04	-13.319	0.653
47000	156.535	4.310e+00	1.443e-04	-14.515	0.302
47500	156.171	4.056e+00	1.361e-04	-15.698	0.318
48000	155.815	3.816e+00	1.284e-04	-16.922	0.314
48500	155.720	3.590e+00	1.208e-04	-18.169	0.288
49000	156.160	3.378e+00	1.134e-04	-19.272	0.787
49500	155.844	3.178e+00	1.069e-04	-19.894	1.811
50000	156.221	2.990e+00	1.003e-04	-19.900	1.801
50500	155.511	2.813e+00	9.482e-05	-19.313	0.802
51000	154.729	2.646e+00	8.964e-05	-20.552	3.094
51500	153.710	2.488e+00	8.485e-05	-22.654	7.092
52000	153.588	2.339e+00	7.983e-05	-24.276	10.254
52500	154.146	2.199e+00	7.478e-05	-25.256	12.327
53000	154.360	2.068e+00	7.022e-05	-25.865	13.783
53500	156.759	1.946e+00	6.505e-05	-25.735	13.843
54000	156.853	1.831e+00	6.120e-05	-25.563	13.849
54500	156.362	1.724e+00	5.779e-05	-25.388	13.849
55000	155.550	1.622e+00	5.467e-05	-25.214	13.848
55500	154.739	1.526e+00	5.171e-05	-25.086	13.857
56000	154.092	1.436e+00	4.884e-05	-24.960	13.865
56500	153.422	1.350e+00	4.613e-05	-24.833	13.871
57000	152.816	1.269e+00	4.354e-05	-24.655	13.914
57500	152.412	1.193e+00	4.103e-05	-24.474	13.956
58000	151.796	1.121e+00	3.871e-05	-24.293	13.995
58500	151.471	1.053e+00	3.645e-05	-24.094	13.805
59000	150.840	9.895e-01	3.439e-05	-23.895	13.603
59500	150.564	9.294e-01	3.236e-05	-23.695	13.403
60000	150.448	8.729e-01	3.041e-05	-23.493	13.281
60500	150.542	8.198e-01	2.854e-05	-23.292	13.166
61000	150.935	7.700e-01	2.674e-05	-23.090	13.051
61500	150.763	7.234e-01	2.515e-05	-22.892	12.786
62000	150.343	6.794e-01	2.369e-05	-22.696	12.501
62500	150.051	6.381e-01	2.229e-05	-22.499	12.220
63000	149.431	5.992e-01	2.102e-05	-22.326	12.135
63500	148.878	5.625e-01	1.980e-05	-22.157	12.094
64000	148.379	5.280e-01	1.865e-05	-21.989	12.052
64500	147.932	4.954e-01	1.755e-05	-21.818	11.972
65000	147.574	4.648e-01	1.651e-05	-21.646	11.878
65500	147.307	4.361e-01	1.552e-05	-21.475	11.784
66000	146.969	4.091e-01	1.459e-05	-21.262	11.613
66500	146.647	3.837e-01	1.371e-05	-21.025	11.400
67000	146.445	3.598e-01	1.288e-05	-20.789	11.189
67500	146.300	3.374e-01	1.209e-05	-20.577	10.984

MOLA Altitude (m)	Temperature (K)	Pressure (Pa)	Density (kg/m^3)	East Wind (m/s)	North Wind (m/s)
68000	146.161	3.164e-01	1.135e-05	-20.386	10.784
68500	146.015	2.967e-01	1.065e-05	-20.196	10.586
69000	145.932	2.782e-01	9.993e-06	-20.016	10.404
69500	145.033	2.608e-01	9.425e-06	-19.854	10.247
70000	145.149	2.444e-01	8.827e-06	-19.692	10.092
70500	145.340	2.291e-01	8.263e-06	-19.517	9.928
71000	145.564	2.148e-01	7.735e-06	-19.303	9.735
71500	145.855	2.014e-01	7.238e-06	-19.090	9.545
72000	146.169	1.889e-01	6.773e-06	-18.887	9.381
72500	146.524	1.771e-01	6.337e-06	-18.816	9.543
73000	146.886	1.662e-01	5.930e-06	-18.743	9.700
73500	147.258	1.559e-01	5.550e-06	-18.667	9.852
74000	147.624	1.463e-01	5.195e-06	-18.544	10.088
74500	147.980	1.373e-01	4.864e-06	-18.415	10.329
75000	148.321	1.289e-01	4.556e-06	-18.284	10.562
75500	148.644	1.210e-01	4.268e-06	-18.144	10.672
76000	148.950	1.137e-01	4.000e-06	-18.000	10.724
76500	149.240	1.067e-01	3.749e-06	-17.855	10.773
77000	149.509	1.003e-01	3.515e-06	-17.684	10.778
77500	149.761	9.419e-02	3.297e-06	-17.482	10.733
78000	149.986	8.850e-02	3.093e-06	-17.281	10.687
78500	150.189	8.316e-02	2.902e-06	-17.091	10.621
79000	150.362	7.814e-02	2.724e-06	-16.933	10.491
79500	150.509	7.344e-02	2.558e-06	-16.775	10.361
80000	150.628	6.902e-02	2.402e-06	-16.617	10.232
80500	150.723	6.488e-02	2.256e-06	-16.438	10.117
81000	150.796	6.099e-02	2.120e-06	-16.258	10.002
81500	150.852	5.733e-02	1.992e-06	-16.078	9.888
82000	150.956	5.389e-02	1.871e-06	-15.921	9.684
82500	151.027	5.067e-02	1.758e-06	-15.774	9.445
83000	151.239	4.764e-02	1.651e-06	-15.626	9.209
83500	151.239	4.479e-02	1.552e-06	-15.446	9.053
84000	151.239	4.212e-02	1.460e-06	-15.221	9.004
84500	151.239	3.960e-02	1.372e-06	-14.998	8.954
85000	151.239	3.724e-02	1.291e-06	-14.779	8.890
85500	151.239	3.502e-02	1.214e-06	-14.581	8.729
86000	151.239	3.293e-02	1.141e-06	-14.384	8.568
86500	151.239	3.096e-02	1.073e-06	-14.187	8.409
87000	151.239	2.912e-02	1.009e-06	-13.985	8.212
87500	151.239	2.738e-02	9.490e-07	-13.783	8.007
88000	151.239	2.575e-02	8.924e-07	-13.581	7.804
88500	151.239	2.422e-02	8.393e-07	-13.392	7.654
89000	151.239	2.277e-02	7.893e-07	-13.218	7.566
89500	151.239	2.142e-02	7.423e-07	-13.044	7.477
90000	151.239	2.014e-02	6.981e-07	-12.869	7.387
90500	151.239	1.894e-02	6.566e-07	-12.676	7.281
91000	151.239	1.782e-02	6.175e-07	-12.484	7.175
91500	151.239	1.676e-02	5.808e-07	-12.292	7.069

MOLA Altitude (m)	Temperature (K)	Pressure (Pa)	Density (kg/m^3)	East Wind (m/s)	North Wind (m/s)
92000	151.239	1.576e-02	5.463e-07	-12.124	6.980
92500	151.239	1.482e-02	5.138e-07	-11.964	6.896
93000	151.239	1.394e-02	4.833e-07	-11.804	6.812
93500	151.239	1.312e-02	4.546e-07	-11.647	6.755
94000	151.239	1.234e-02	4.276e-07	-11.494	6.752
94500	151.239	1.160e-02	4.022e-07	-11.340	6.746
95000	151.239	1.092e-02	3.783e-07	-11.186	6.737
95500	151.239	1.027e-02	3.559e-07	-11.011	6.644
96000	151.239	9.659e-03	3.348e-07	-10.834	6.545
96500	151.239	9.086e-03	3.149e-07	-10.658	6.445
97000	151.239	8.547e-03	2.962e-07	-10.486	6.349
97500	151.239	8.041e-03	2.787e-07	-10.320	6.257
98000	151.239	7.564e-03	2.622e-07	-10.154	6.164
98500	151.239	7.116e-03	2.466e-07	-9.987	6.072
99000	151.239	6.695e-03	2.320e-07	-9.817	5.994
99500	151.239	6.299e-03	2.183e-07	-9.647	5.915
100000	151.239	5.926e-03	2.054e-07	-9.476	5.834
100500	151.239	5.575e-03	1.932e-07	-9.306	5.748
101000	151.239	5.245e-03	1.818e-07	-9.136	5.656
101500	151.239	4.935e-03	1.710e-07	-8.965	5.564
102000	151.239	4.643e-03	1.609e-07	-8.799	5.479
102500	151.239	4.369e-03	1.514e-07	-8.667	5.464
103000	151.239	4.111e-03	1.425e-07	-8.534	5.446
103500	151.239	3.868e-03	1.341e-07	-8.399	5.423
104000	151.239	3.640e-03	1.261e-07	-8.085	5.617
104500	151.239	3.425e-03	1.187e-07	-7.667	5.936
105000	151.239	3.223e-03	1.117e-07	-7.260	6.235
105500	151.239	3.032e-03	1.051e-07	-6.903	6.426
106000	151.239	2.854e-03	9.890e-08	-6.915	5.799
106500	151.239	2.685e-03	9.307e-08	-6.919	5.196
107000	151.239	2.527e-03	8.758e-08	-6.914	4.616
107500	151.239	2.378e-03	8.242e-08	-6.808	4.306
108000	151.239	2.238e-03	7.756e-08	-6.628	4.193
108500	151.239	2.106e-03	7.299e-08	-6.449	4.079
109000	151.239	1.982e-03	6.870e-08	-6.269	3.974
109500	151.239	1.865e-03	6.465e-08	-6.018	4.467
110000	151.239	1.756e-03	6.085e-08	-5.772	4.924
110500	151.239	1.652e-03	5.727e-08	-5.529	5.344
111000	151.239	1.555e-03	5.390e-08	-5.346	5.234
111500	151.239	1.464e-03	5.073e-08	-5.227	4.528
112000	151.239	1.378e-03	4.775e-08	-5.105	3.857
112500	151.239	1.297e-03	4.494e-08	-4.978	3.223
113000	151.239	1.220e-03	4.230e-08	-4.797	3.036
113500	151.239	1.149e-03	3.981e-08	-4.607	2.917
114000	151.239	1.081e-03	3.748e-08	-4.418	2.799
114500	151.239	1.018e-03	3.528e-08	-4.228	2.670
115000	151.239	9.581e-04	3.321e-08	-4.041	2.515
115500	151.239	9.019e-04	3.126e-08	-3.853	2.363

MOLA Altitude (m)	Temperature (K)	Pressure (Pa)	Density (kg/m^3)	East Wind (m/s)	North Wind (m/s)
116000	151.239	8.490e-04	2.942e-08	-3.665	2.214
116500	151.239	7.992e-04	2.770e-08	-3.477	2.089
117000	151.239	7.524e-04	2.608e-08	-3.289	1.977
117500	151.239	7.083e-04	2.455e-08	-3.102	1.864
118000	151.239	6.668e-04	2.311e-08	-2.914	1.751
118500	151.239	6.277e-04	2.176e-08	-2.720	1.603
119000	151.239	5.910e-04	2.048e-08	-2.526	1.460
119500	151.239	5.564e-04	1.928e-08	-2.333	1.321
120000	151.239	5.238e-04	1.815e-08	-2.142	1.199
120500	151.239	4.932e-04	1.709e-08	-1.953	1.102
121000	151.239	4.643e-04	1.609e-08	-1.765	1.004
121500	151.239	4.372e-04	1.515e-08	-1.577	0.905
122000	151.239	4.116e-04	1.427e-08	-1.394	0.791
122500	151.239	3.875e-04	1.343e-08	-1.212	0.673
123000	151.239	3.649e-04	1.265e-08	-1.030	0.559
123500	151.239	3.436e-04	1.191e-08	-0.847	0.450
124000	151.239	3.235e-04	1.121e-08	-0.663	0.352
124500	151.239	3.046e-04	1.056e-08	-0.480	0.255
125000	151.239	2.869e-04	9.942e-09	-0.296	0.157